ISSN : 0974 - 7486 Volume 14 Issue 12

Materials Science

An Indian Journal

Full Paper

MSAIJ, 14(12), 2016 [514-526]

Electrochemical corrosion behavior, hardness andthermal propertiesofcopper based alloys

Abu Bakr El-Bediwi[1]*, S.Bader[1], Zuhor Farag[2]

[1]Metal Physics Lab., Physics Department, Faculty of Science, Mansoura University, (EGYPT)

[2]Faculty of Education Janzor, University of Tripoli, (LIBYA)

E-mail: baker_elbediwi@yahoo.com

ABSTRACT

Modified copper (high copper based alloys) are used in structural parts and friction materials. The aim of this study was to evaluate the effect of adding small amount of Al, Ge, Mn, Ni and Sn on microstructure, electrochemical corrosion behavior, hardness and thermal properties of copper. Crystal size of Cu decreased but lattice microstrain increasedafter adding small amount of Al, Ge, Mn, Ni. Corrosion resistance of Cu decreased after adding Al, Ge, Mn, Ni and Sn. Nickel, Germanium and tin have a high lattice microstrain and lowest corrosion rate. Differential scanning calorimeter shows a change in endothermal peak of copper based alloys which correlated to alloy composition and that is agreed with x-ray and scanning electron microscope analysis. A significant increase in copper strength after adding small amount of Al, Ge, Mn, Ni and Sn especially Sn element.

KEYWORDS

Corrosion rate;
Hardness;
Lattice microstrain;
Microstructure;
Copper alloys.

INTRODUCTION

Copper alloys are metal alloys that have copper as their principal component. In modern industry there are many different types of copper and copper alloy are used and their compositions roughly grouped into the categories: copper, high copper alloy, brasses, bronzes, copper nickels, copper–nickel–zinc, leaded copper and special alloys. High copper alloys contain small amounts of various alloying elements such as beryllium, chromium, zirconium, tin, silver, sulfur or iron. These elements modify one or more of the basic properties of copper, such as strength, creep resistance, machinability or weldability. Most of the uses are similar to those given above for coppers, but the conditions of application are more extreme. The influence of heat treatment on its shape-memory effect of Cu-Zn-Al ternary alloy was examined[1]. The shape-memory effect is strongly influenced by many heat-treatment parameters, such as betatizing temperature, betatizing duration and rate of quenching. Various additions showed effective on grain refinement of different copper alloys. For bronzes and gun metals, 0.3% Zr with C and or N in the absence of sulfur, 0.2% Ti with 0.03% B and 0.1% Fe or Co with 0.03% B are effective. Zirconium effective in tin bronzes and red brass but it is not silicon bronze. Although sulfur destroys the grain refining effect of zirconium and it could be recovered by adding magnesium[2]. Adding

0.05% Zr or 1% iron is effective for gun metals and red brass. Iron was effective as grain refiner for aluminum and manganese bronzes. Iron-free aluminum bronzes and beta brasses can be refined by a combination of 0.03% Zr and 0.02% B[3]. Zirconium (0.3%) and boron (0.02%) together were effective in Fe-free beta brass[4]. Adding hard particles such as SiC, Al_2O_3, TiB_2 and TiC significantly improve the mechanical properties of copper matrix materials while maintaining high electrical and thermal conductivity[5-7]. The combination of ceramic particles as reinforcement may also enhance the high temperature mechanical properties, oxidation and wear resistance, without severe worsening of thermal and electrical conductivity of the copper matrix. Low price Al_2O_3 particles have mostly selected as the reinforcement phase[8, 9]. Also the uniform distribution of Al_2O_3 particles can be accomplished by the process of internal oxidation[10, 11] or by mechanical alloying[12, 13]. Pure copperis used in the electrical and the electronics industries because of its excellent electrical and thermal conductivities. The aim of our research was to improve some physical properties (such as strength, creep resistance, machinability or weldability) by adding alloying elements such as aluminum, tin, nickel, manganese and germanium with minor concentration. This research is important because modified copper (high copper based alloys) are used in structural parts and friction materials.

EXPERIMENTAL METHODS

Commercial bare of copper sheet (purity 99.9%) and $Cu_{98}Sn_2$ (98 wt. % Cu and 2wt. % Sn), $Cu_{98}Al_2$ (98 wt. % Cu and 2 wt. % Al), $Cu_{98}Ni_2$ (98 wt. % Cu and 2 wt. % Ni), $Cu_{98}Mn_2$ (98 wt. % Cu and 2 wt. % Mn) and $Cu_{98}Ge_2$ (98 wt. % Cu and 2 wt. % Ge) alloys were provided via the European Copper Institute, Brussels. The bare samples were cut to suiTABLE dimensions for different measurements. Microstructure of used samples was studied using a Shimadzu x–ray diffractometer (Dx–30, Japan)and scanning electron microscope(JEOL JSM-6510LV, Japan). A digital Vickers micro-hardness tester, (Model-FM-7- Japan), was used to measure Vickers hardness values of used alloys. The polarization studies were performed using Gamry Potentiostat/ Galvanostat with a Gamry framework system based on ESA 300. Gamry applications include software DC105 for corrosion measurements, and Echem Analyst version 5.5 softwarepackages for data fitting. The working electrode was immersed in the acid solution and the constant steady-state (open circuit) potential was recorded when it became virtually constant. The polarization studies were carried out over a potential of +250 to -250 mV with respect to the open circuit potential at a scan rate of 5 mV s^{-1}. The linear Tafel segments of the anodic and cathodic curves were extrapolated to obtain corrosion potential (E_{corr}) and corrosion current density (j_{corr}). DSC measurements above room temperature of used samples were performed using SDT Q600 (V20.9 Build 20) instrument, U. S. A.

RESULTS AND DISCUSSION

Microstructure analysis

X-ray diffraction analysis

X-ray diffraction patterns of Cu metal, $Cu_{98}Ge_2$,$Cu_{98}Mn_2$, $Cu_{98}Al_2$, $Cu_{98}Sn_2$, and $Cu_{98}Ni_2$ alloys have lines corresponding to Cu face centered cubic with Cu_2O(Copper contain Oxygen content, Oxygen is almost insoluble in Cu and forms Cu_2O)\ or and intermetallic phase contain Cu and one of alloying elements as shown in Figure 1 (a, b, c, d, e and f). That is meant that, some atoms of Sn or Al or Ni or Mn or Ge dissolved in Cu matrix and other atoms formed CuSn or CuAl or CuNi or CuMn or CuGe intermediate phase with different compositions. The details of x-ray analysis for Cu metal, $Cu_{98}Ge_2$, $Cu_{98}Mn_2$, $Cu_{98}Al_2$, $Cu_{98}Sn_2$and $Cu_{98}Ni_2$alloys are listed in TABLE 1 (a, b, c, d, e and f). From these analyses it is obvious that, small amounts of an alloying element added to molten copper will completely dissolve and form a homogeneous microstructure (a single phase). But at some point, additional amounts of the alloying element will not dissolve; the exact amount is dependent on the solid solubility of the particular element in copper. When that solid solubility limit is exceeded, two distinct microstructures form with different composi-

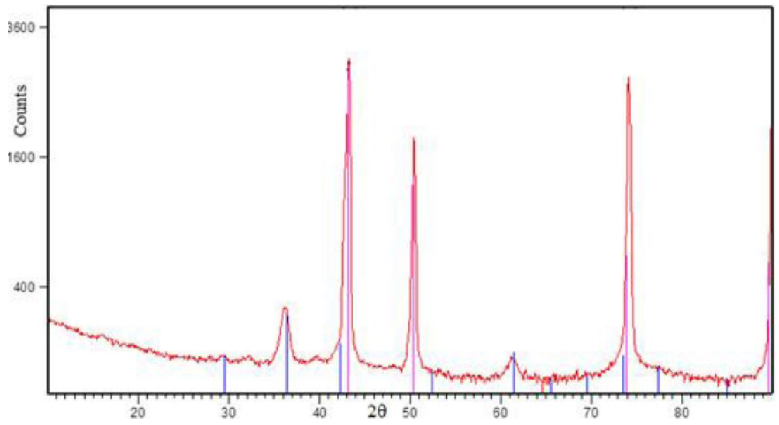

Figure (1a) : X-ray diffraction patterns of pure copper

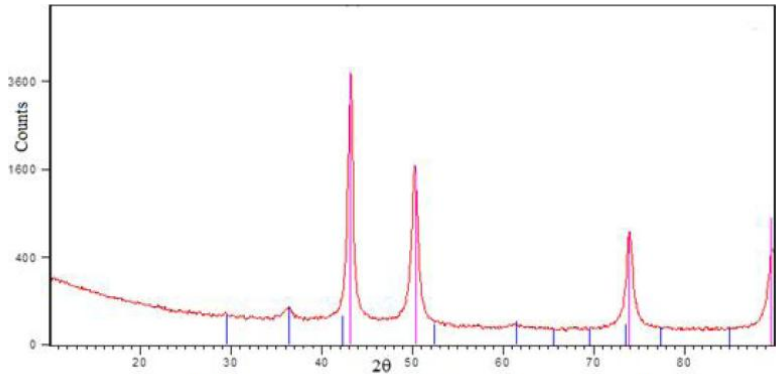

Figure (1b) : X-ray diffraction patterns of $Cu_{98}Ge_2$ alloy

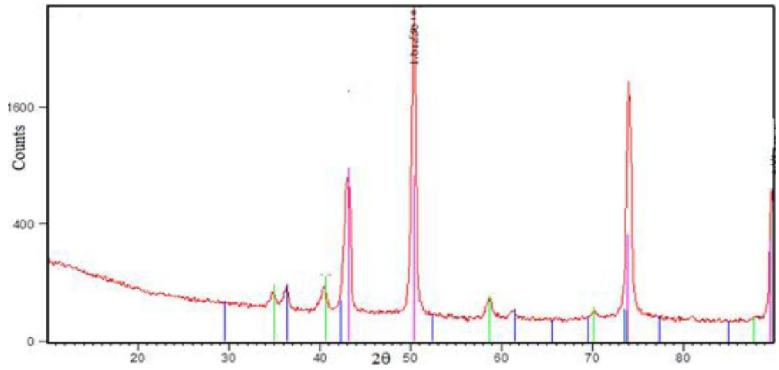

Figure (1c) : X-ray diffraction patterns of $Cu_{98}Mn_2$alloy

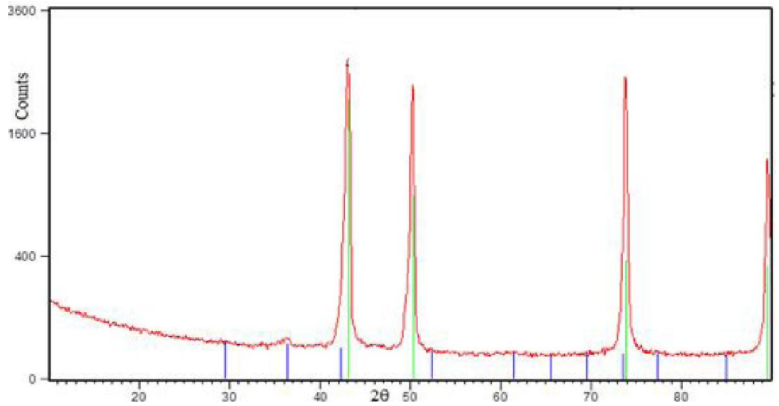

Figure (1d) : X-ray diffraction patterns of $Cu_{98}Al_2$alloy

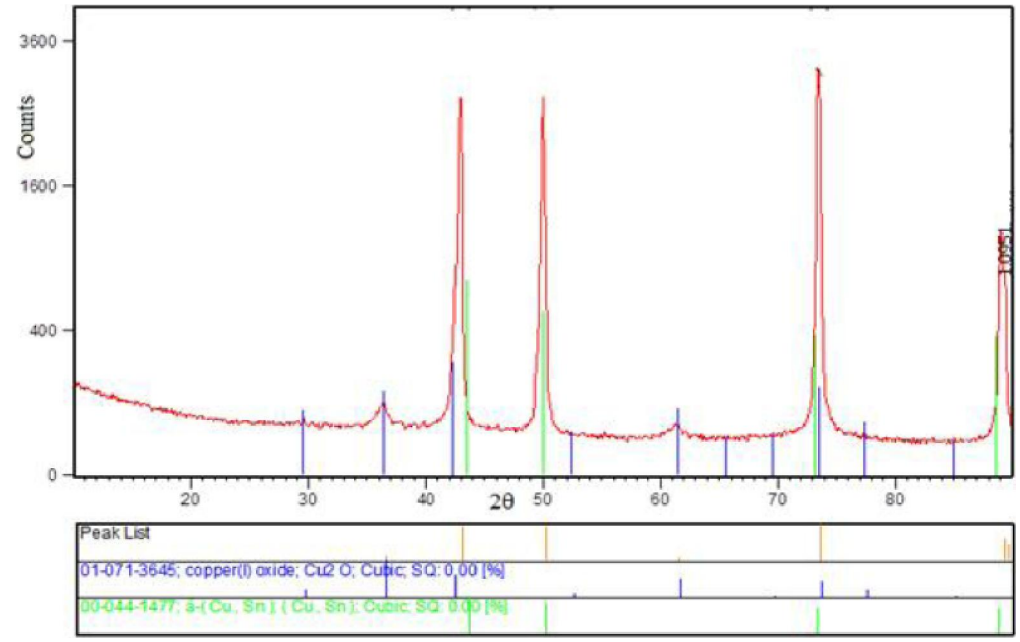

Figure (1e) : X-ray diffraction patterns of $Cu_{98}Sn_2$alloy

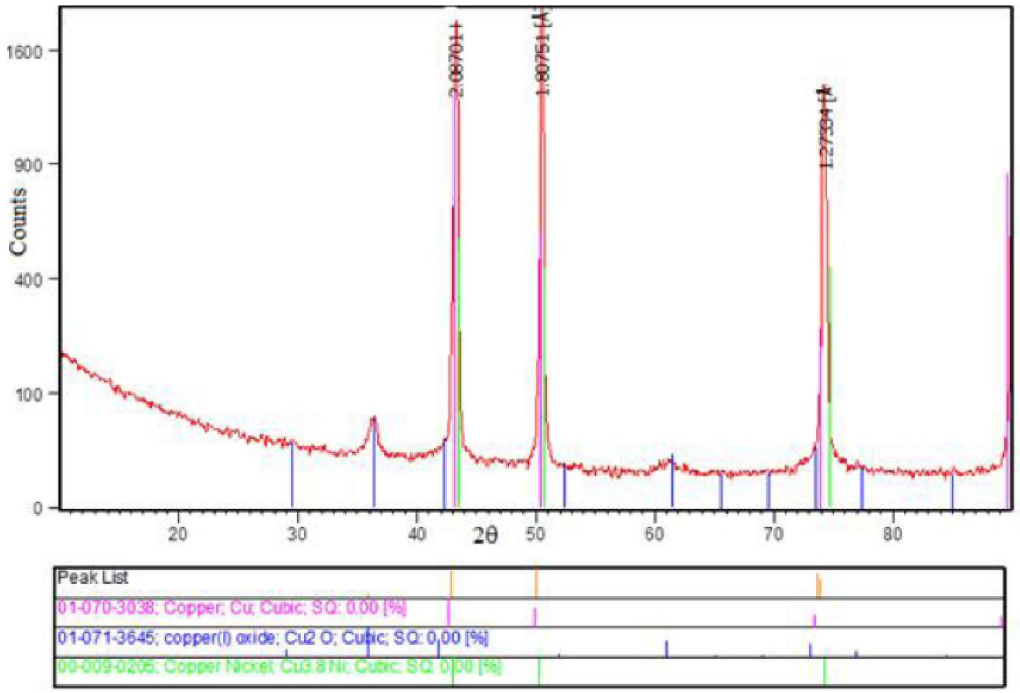

Figure (1f) : X-ray diffraction patterns of $Cu_{98}Ni_2$alloy

TABLE (1a) : X-ray analysis of pure Cu

2θ	d Å	Int. %	FWHM	Area	Phase	hkl
36.1944	2.48185	5.79	0.7085	120.84	Cu_2O	111
43.2549	2.0917	100	0.1378	405.82	Cu	111
50.3991	1.81068	57.17	0.3346	563.46	Cu	200
61.3214	1.51178	0.87	0.7872	20.16	Cu_2O	220
74.1106	1.27832	87.15	0.288	999.41	Cu	220

tions. Lattice parameters, (a and c), unit volume cell and crystal size of Cu phase in Cu metal and $Cu_{98}X_2$

Full Paper

TABLE (1b) : X-ray analysis of $Cu_{98}Ge_2$ alloy

2θ	d Å	Int. %	FWHM	Area	Phase	hkl
36.3984	2.46841	1.1	0.6298	24.63	Cu_2O	111
43.2646	2.09125	100	0.4133	1466.42	Cu	111
50.3247	1.81318	44.82	0.3936	625.92	Cu	200
73.8939	1.28153	17.7	0.288	244.46	Cu	220

TABLE (1c) : X-ray analysis of $Cu_{98}Mn_2$ alloy

2θ	d Å	Int. %	FWHM	Area	Phase	hkl
34.846	2.57473	1.07	0.6298	21.53	CuMn	
36.3915	2.46886	1.62	0.4723	24.36	Cu_2O	111
40.6248	2.22083	1.53	0.4723	23.05	CuMn	
43.1918	2.09461	22.48	0.2362	169.49	Cu	111
50.349	1.81236	100	0.3936	1256.72	Cu	200
58.7363	1.572	1.2	0.551	21.08	CuMn	
61.2382	1.51364	0.33	0.9446	10.05	Cu_2O	220
73.976	1.28138	58.47	0.2952	551.07	Cu	200
89.7605	1.09165	20.42	0.264	232.64	Cu	311

TABLE (1d) : X-ray analysis of $Cu_{98}Al_2$ alloy

2θ	d Å	Int. %	FWHM	Area	Phase	hkl
36.25	2.47817	0.28	0.09	0.6	Cu_2O	111
43.163	2.09594	100	0.3149	1111.47	Cu	111
50.2148	1.81689	61.4	0.3346	725.1	Cu	200
73.7701	1.28444	64.9	0.2952	676.3	Cu	220
89.5338	1.09383	34.91	0.336	559.64	Cu	311

TABLE (1e) : X-ray analysis of $Cu_{98}Sn_2$ alloy

2θ	d Å	Int. %	FWHM	Area	phase	hkl
36.3087	2.4743	1.73	0.6298	33.31	Cu_2O	111
42.954	2.10565	86.92	0.3346	891.61	Cu	111
49.9872	1.82463	87.16	0.3149	841.44	Cu	200
61.2923	1.51243	0.66	0.9446	19.24	Cu_2O	220
73.4219	1.28967	100	0.3346	1025.78	Cu	220
89.0202	1.09971	35.27	0.2558	276.66	Cu	311
89.3947	1.09517	18.9	0.216	169.16	Cu	311

TABLE (1f) : X-ray analysis of$Cu_{98}Ni_2$ alloy

2θ	d Å	Int. %	FWHM	Area	phase	hkl
36.4602	2.46437	1.9	0.4723	16.9	Cu_2O	111
43.357	2.08701	90.02	0.4133	699.38	Cu	111
50.4938	1.80751	100	0.3149	591.92	Cu	200
74.1782	1.27838	69.83	0.2362	309.99	Cu	220
74.4498	1.27334	38.7	0.192	188.79	Cu	111

(Ge or Mn or Al or Sn or Ni)alloys were determined and then listed in TABLE (1g). Also from the relation between full width half maximum (β) and 4tanθ as shown in Figure (1h), the induced internal lattice microstrain of Cu metal and $Cu_{98}X_2$ (Ge or Mn or Al or Sn or Ni)alloyswere calculated and

TABLE (1g) : Lattice parameter, unit cell volume and crystal size of $Cu_{98}X_2$ alloys

Alloys	a Å	V Å^3	τ Å
Pure Cu	4.299	79.434	409
$Cu_{98}Ge_2$	3.622	47.523	258
$Cu_{98}Mn_2$	4.442	87.627	289
$Cu_{98}Al_2$	4.292	79.082	301
$Cu_{98}Sn_2$	4.286	78.712	357
$Cu_{98}Ni_2$	3.615	47.234	357

TABLE (1h) : Lattice strain of$Cu_{98}X_2$ alloys

Alloys	Lattice strain (ε)× 10^{-4}
Pure Cu	7
$Cu_{98}Ge_2$	28
$Cu_{98}Mn_2$	11
$Cu_{98}Al_2$	9
$Cu_{98}Sn_2$	19
$Cu_{98}Ni_2$	24

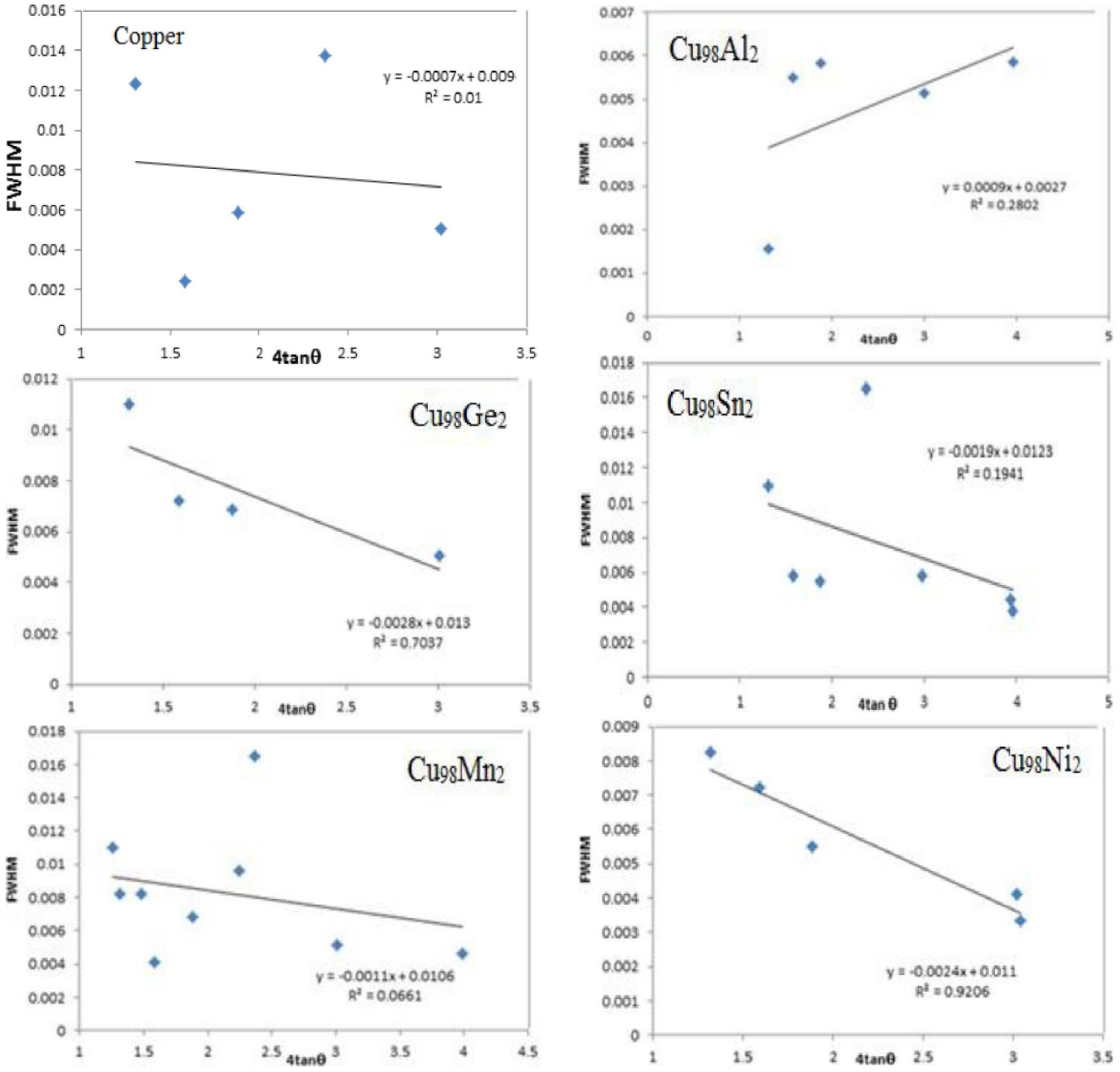

Figure 1(g) : FWHM versus 4tanθ for $Cu_{98}X_2$ alloys

then listed in TABLE (1h).

Scanning electron micrographs and EDX analysis

Figure 2(a- f) shows scanning electron micrographs, SEM, and EDX of Cu metal and $Cu_{98}X_2$ (Ge

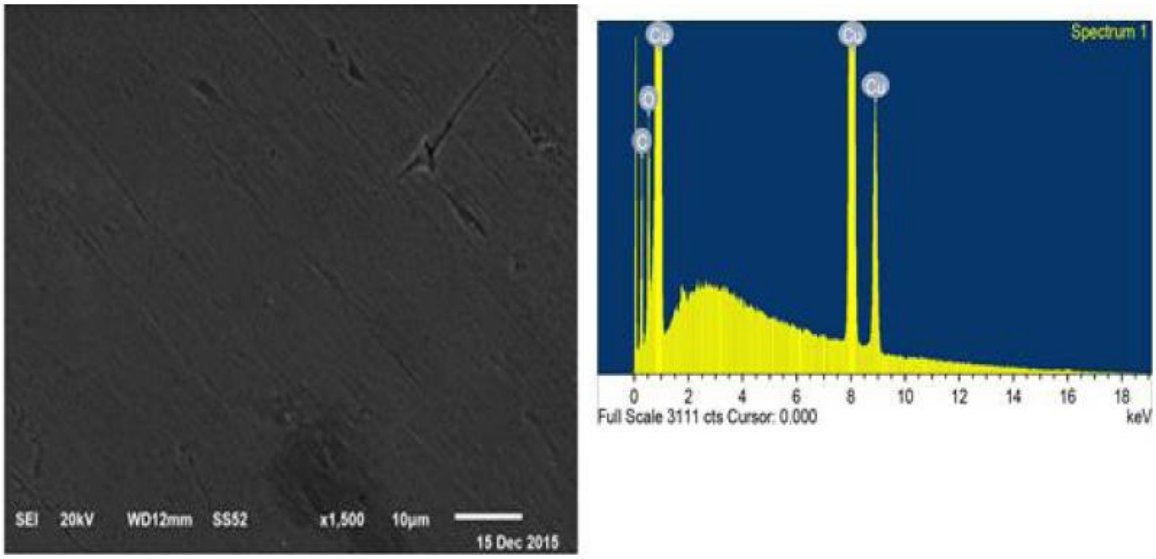

Figure (2a) : SEM and EDX of pure copper

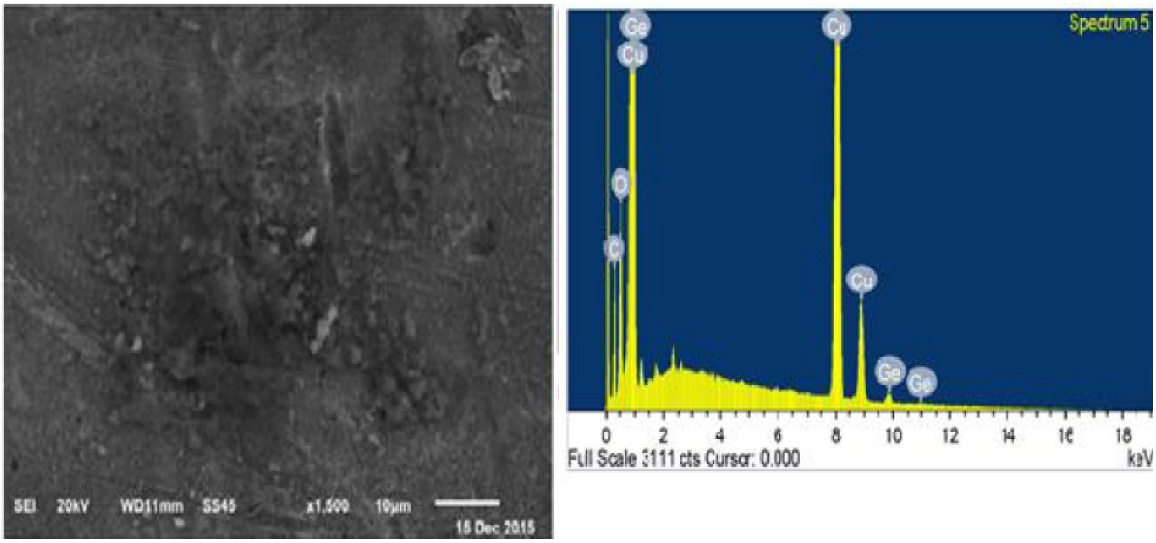

Figure (2b) : SEM and EDX of $Cu_{98}Ge_2$ alloy

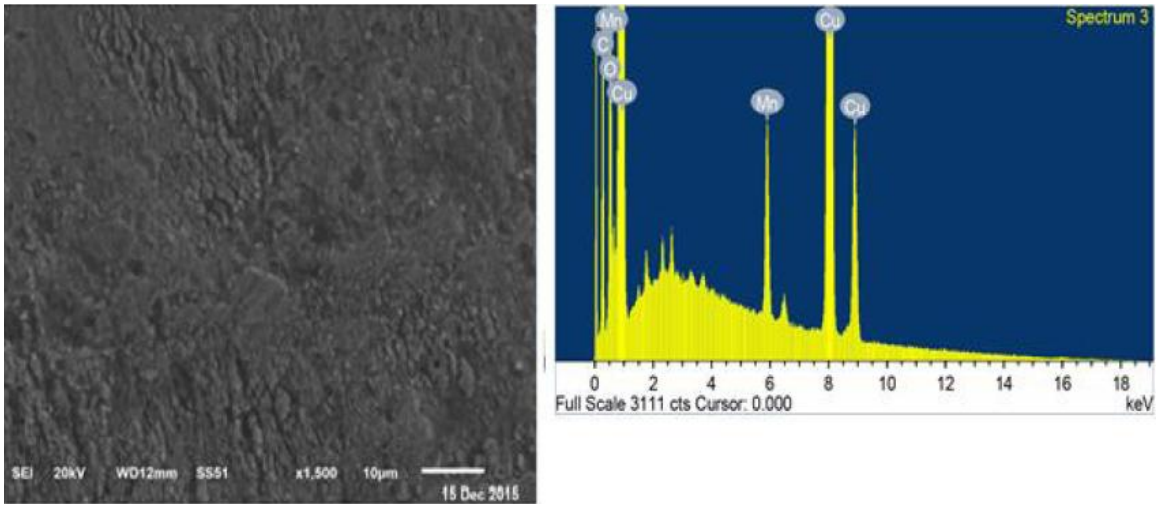

Figure (2c) : SEM and EDX of $Cu_{98}Mn_2$ alloy

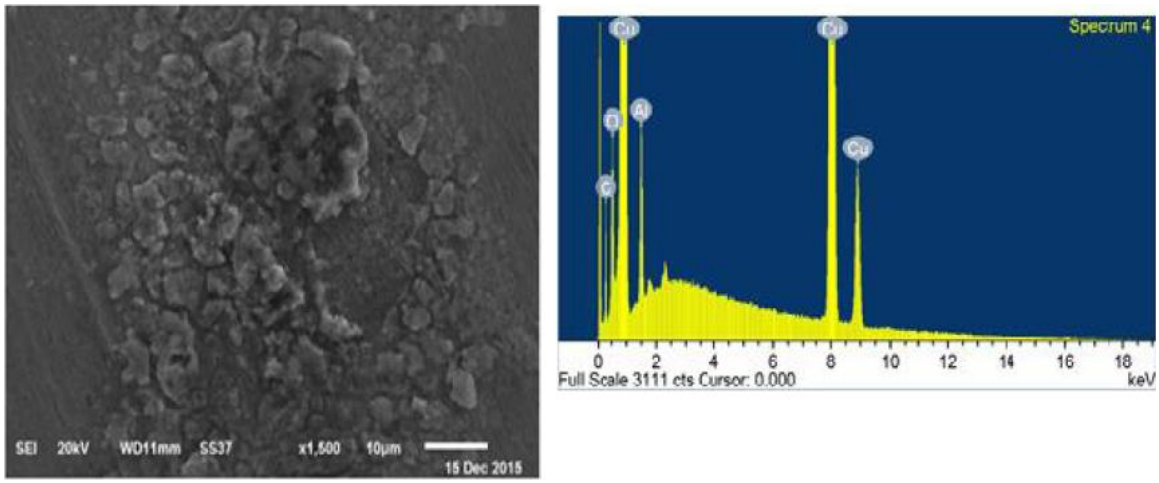

Figure (2d) : SEM and EDX of $Cu_{98}Al_2$ alloy

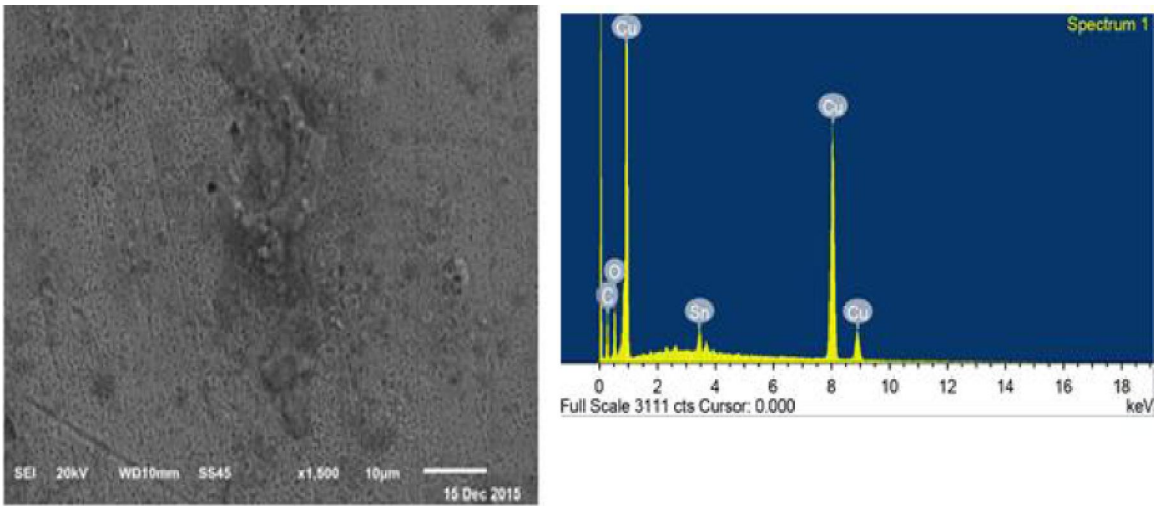

Figure (2e) : SEM and EDX of $Cu_{98}Sn_2$ alloy

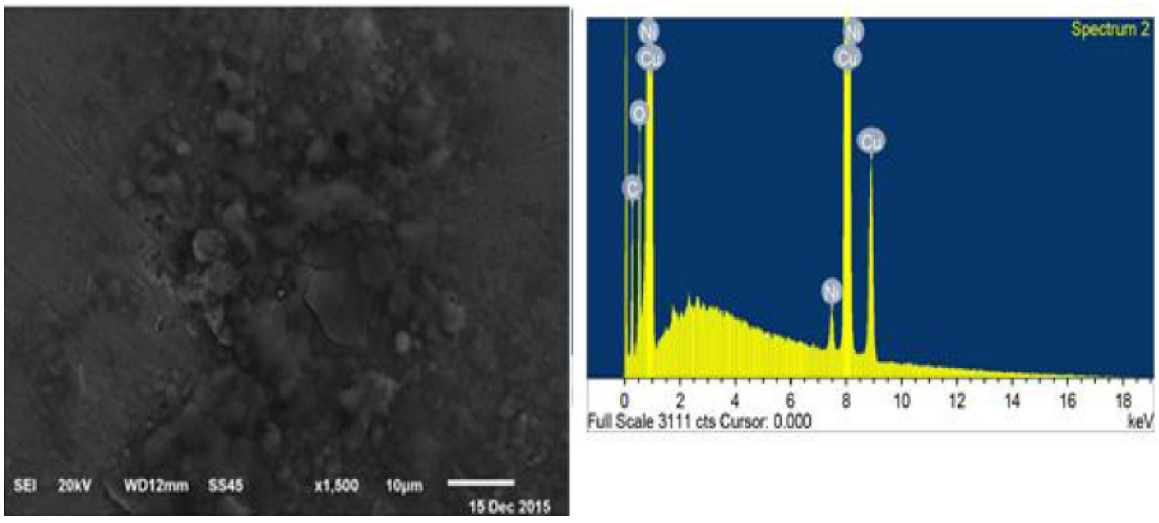

Figure (2f) : SEM and EDX of $Cu_{98}Ni_2$ alloy

or Mn or Al or Sn or Ni) alloyswhich have heterogeneity structure. Figure (2b) shows germanium-copper/ or germanium grains disturbed in Cu matrix as different rod size, shape and orientation with small grains and strips. But EDX analysis show Cu, O, C and Ge atoms appeared in $Cu_{98}Ge_2$ alloy. Manga-

Full Paper

TABLE 2 : Vickers hardness and maximum shear stress of$Cu_{98}X_2$ alloys

Alloys	H_v kg/mm^2	μ_n kg/mm^2
Pure Cu	28.475±1.78	9.4
$Cu_{98}Ge_2$	43.55±5.5	14.37
$Cu_{98}Mn_2$	44.475±3.17	14.68
$Cu_{98}Al_2$	50.55±6.63	16.68
$Cu_{98}Sn_2$	69.675±5.58	22.99
$Cu_{98}Ni_2$	45±0.5	14.85

nese-copper/ or Manganese grains disturbed in Cu matrix as homogenous narrow dendritic e with small grains ~0.5µm. But EDX analysis show Cu, O, C and Mn atoms appeared in $Cu_{98}Mn_2$ alloy as shown in Figure (2c). Figure (2d) shows aluminum-copper/ or aluminum grains disturbed in Cu matrix as circular shape like dendrite with different size from ~1µm to 20 µm and strip with ~ 10 µm. But EDX analysis show Cu, O, C and Al atoms appeared in $Cu_{98}Al_2$ alloy. Tin-copper/ or tin grains disturbed in Cu matrix at different position with different size from ~1µm to 3 µm and dendrite shape with ~12 µm and strip with ~ 1 µm. But EDX analysis show Cu, O, C and Sn atoms appeared in $Cu_{98}Sn_2$ alloy as shown in Figure (2e). Figure (2f) shows nickel atoms disturbed in Cu matrix as dendrite shape with different grain size from ~ 3 µm to 30 µm and some non homogeneous nickel grain disturbed in matrix.

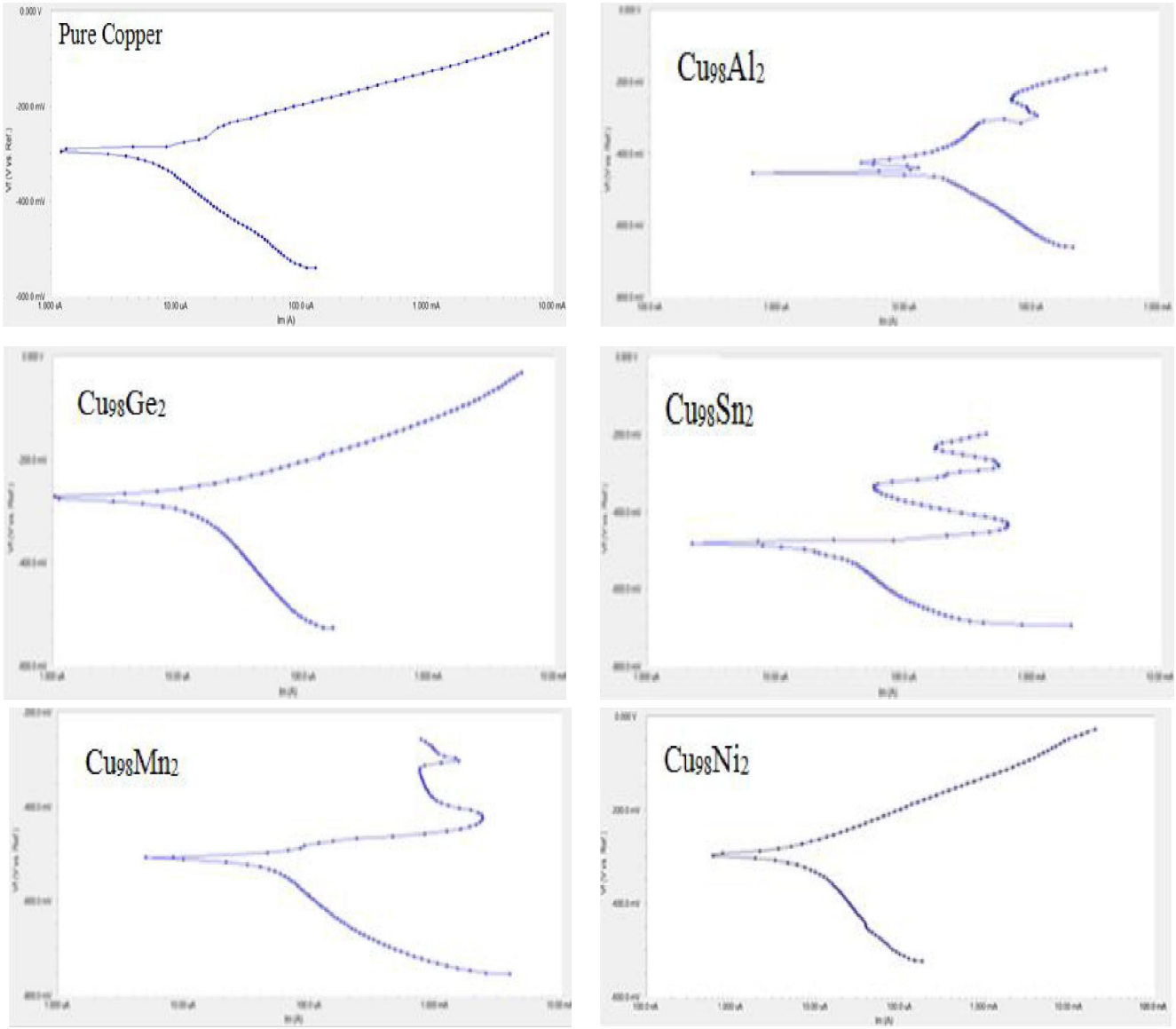

Figure 3 : Electrochemical polarization curves for$Cu_{98}X_2$ alloys

TABLE 2 : Corrosion potential (E_{Corr}), corrosion current (I_{Corr}), and corrosion rate (C. R)of$Cu_{98}X_2$ alloys

Alloys	$-E_{corr}$mV	I_{corr}µA cm^{-2}	C. R mpy
Pure Cu	293	5.89	2.994
$Cu_{98}Ge_2$	273	9.93	5.042
$Cu_{98}Mn_2$	509	60	30.47
$Cu_{98}Al_2$	454	46.6	23.68
$Cu_{98}Sn_2$	481	15.4	7.807
$Cu_{98}Ni_2$	296	8.71	4.424

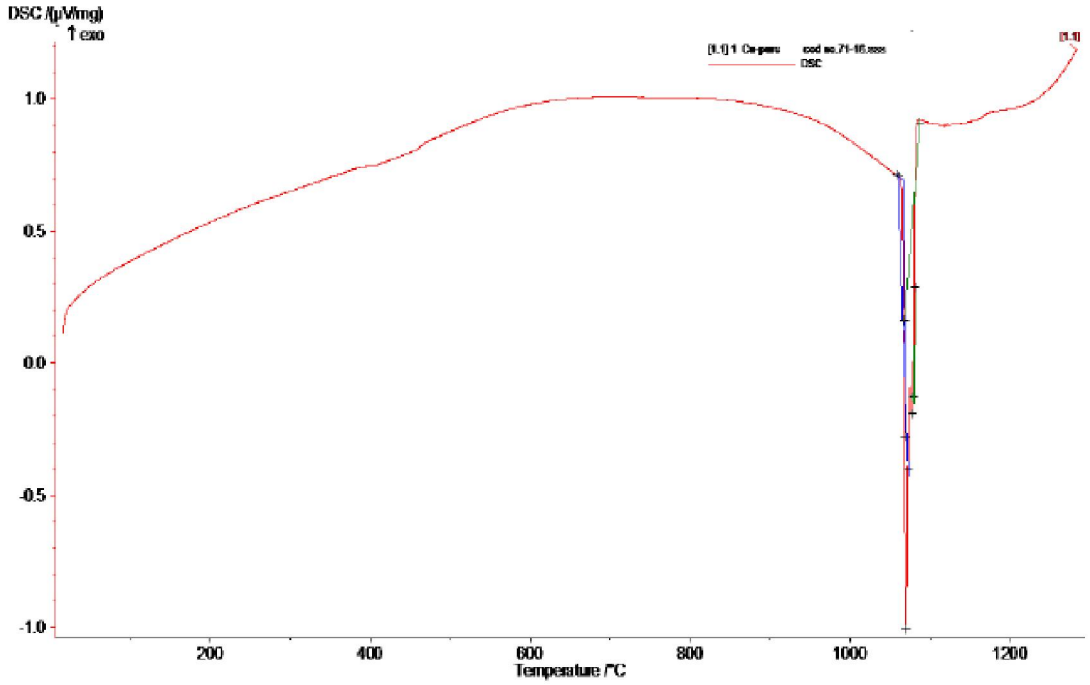

Figure (4a) : DSC thermograph of pure copper

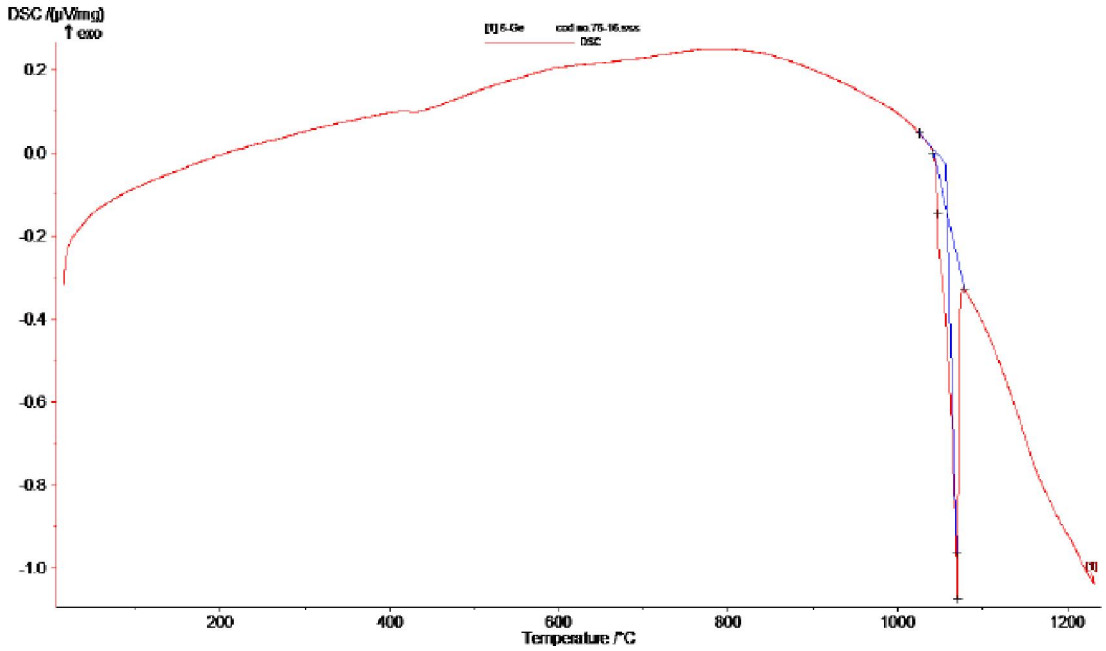

Figure (4b) : DSC thermograph of $Cu_{98}Ge_2$ alloy

Full Paper

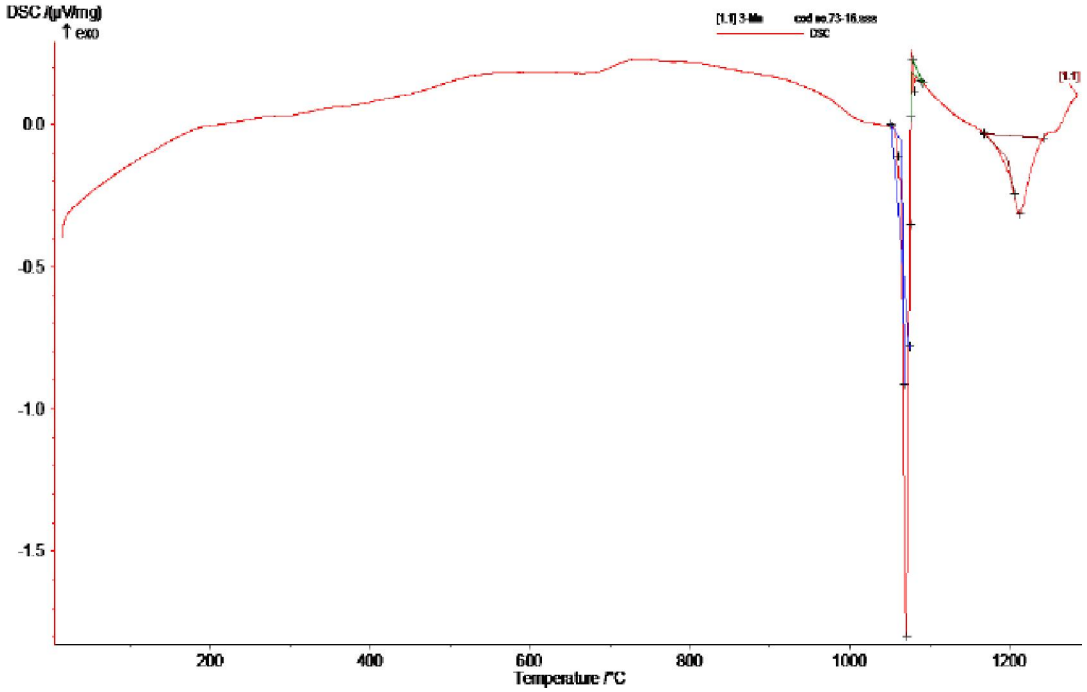

Figure (4c) : DSC thermographof$Cu_{98}Mn_2$ alloy

Also strip with ~ 15 µm of Cu grains appeared. But EDX analysis show Cu, O, C and Ni atoms appeared in $Cu_{98}Ni_2$ alloy. These results analysis show that, microstructure of Cu metal, $Cu_{98}Ge_2$, $Cu_{98}Mn_2$, $Cu_{98}Al_2$, $Cu_{98}Sn_2$and $Cu_{98}Ni_2$ alloys showsCu matrix with other phases have different shape andorientation which agreed with x-ray results.

Vickers microhardness and minimum shear stress

The hardness is the property of material, which gives it the ability to resist being permanently deformed when a load is applied. Vickers hardness of $Cu_{98}X_2$ (Ge or Mn or Al or Sn or Ni) alloys at 10 gram force and indentation time 5 sec are listed in TABLE (2). The maximum shear stress (μ_m) value of $Cu_{98}X_2$ (Ge or Mn or Al or Sn or Ni) alloys was calculated using the equation (1)[14], where $\nu$is Poisson's ratio of the elements in the alloy and then listed in TABLE (2).

$$\mu_m = \frac{1}{2} H_\nu \left\{ \frac{1}{2}(1-2\nu) + \frac{2}{9}(1+\nu)[2(1+\nu)]^{\frac{1}{2}} \right\} \quad \textbf{(1)}$$

The results show that, a significant change in Vickers hardness value of copper after adding Ge or Mn or Al or Sn or Ni. That is because these alloying elements formed hard inclusion in Cu matrix with refinement crystal size of it.

Electrochemical corrosion behavior

Figure (3) shows electrochemical polarization curves ofCu metal and $Cu_{98}X_2$ (Ge or Mn or Al or Sn or Ni) alloys in 0.25 M HCl. From these results, the corrosion potential of the Cu metal, and $Cu_{98}X_2$ (Ge or Mn or Al or Sn or Ni) alloysexhibited a negative potential. The cathodic and the anodic polarization curves also showed similar corrosion trends with a variation in shape and position. Cathodic and anodic polarization curves of Mn or Al or Sn have different feature compared to pure copper. The corrosion potential (E_{Corr}), corrosion current (I_{Corr}), and corrosion rate (C. R) of Cu metal and $Cu_{98}X_2$ (Ge or Mn or Al or Sn or Ni) alloys in 0.25 M HCl are presented in TABLE (3). The results show that, the corrosion rate of Cu metal in 0.25 M HCl increased after adding Ge or Mn or Al or Sn or Ni. That is because Ge or Mn or Al or Sn or Ni content caused a heterogeneous microstructure (formed a solid solution with other traces of phases)which effected on microsegregation and reactivity of Cu and Ge or Mn or Al or Sn or Ni atoms with HCl solution.

Thermal behavior

Thermal analysis is regularly used to study solid state transformations as well as solid-liquid reac-

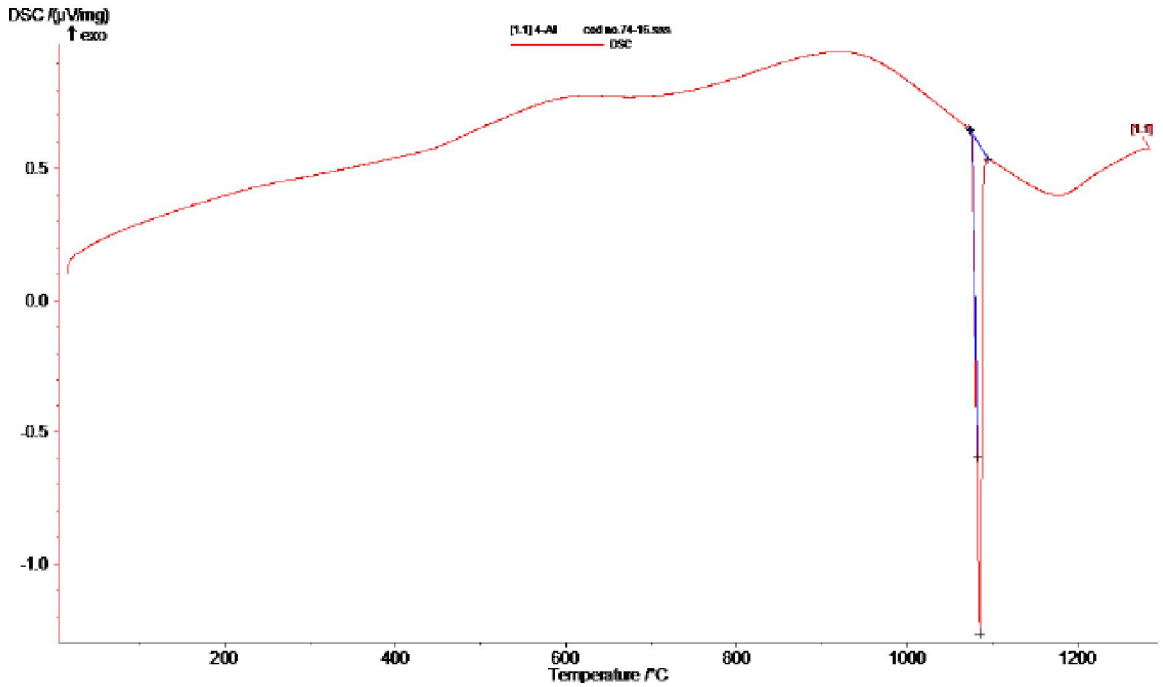

Figure (4d) : DSC thermographof$Cu_{98}Al_2$ alloy

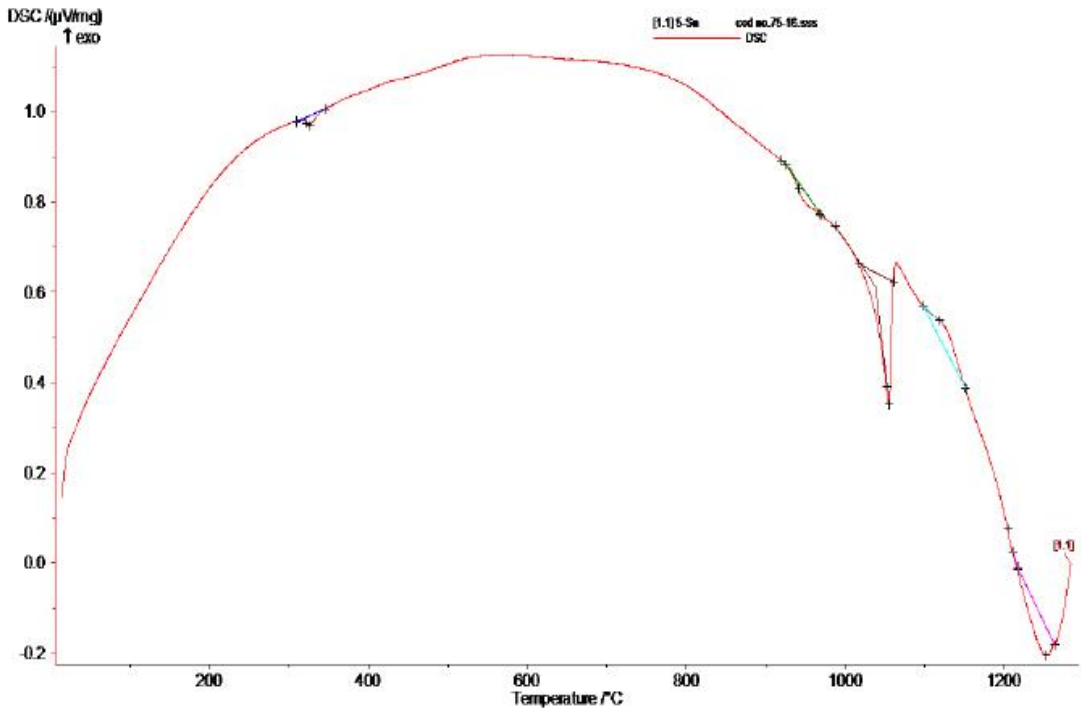

Figure (4e) : DSC thermographof$Cu_{98}Sn_2$ alloy

tions. The magnitudes of thermal properties depend on the nature of solid phase and on its temperature. The differential scanning calorimetry (DSC) thermographs were obtained by SDT Q600 (V20.9 Build 20) with heating rate 10 °C /min in the temperature range 0- 1300 °C.

DSC thermographs of Cu metal and $Cu_{98}X_2$ (Ge or Mn or Al or Sn or Ni)alloys are shown in Figure 4(a- f). From these graphs the melting point of Cu metal, and $Cu_{98}X_2$ (Ge or Mn or Al or Sn or Ni) alloysare identified. Thermo-graph (Endothermal peak) of copper has variations in their shape and position. That means that, there is a change in copper matrix structure caused after adding Ge or Mn

Full Paper

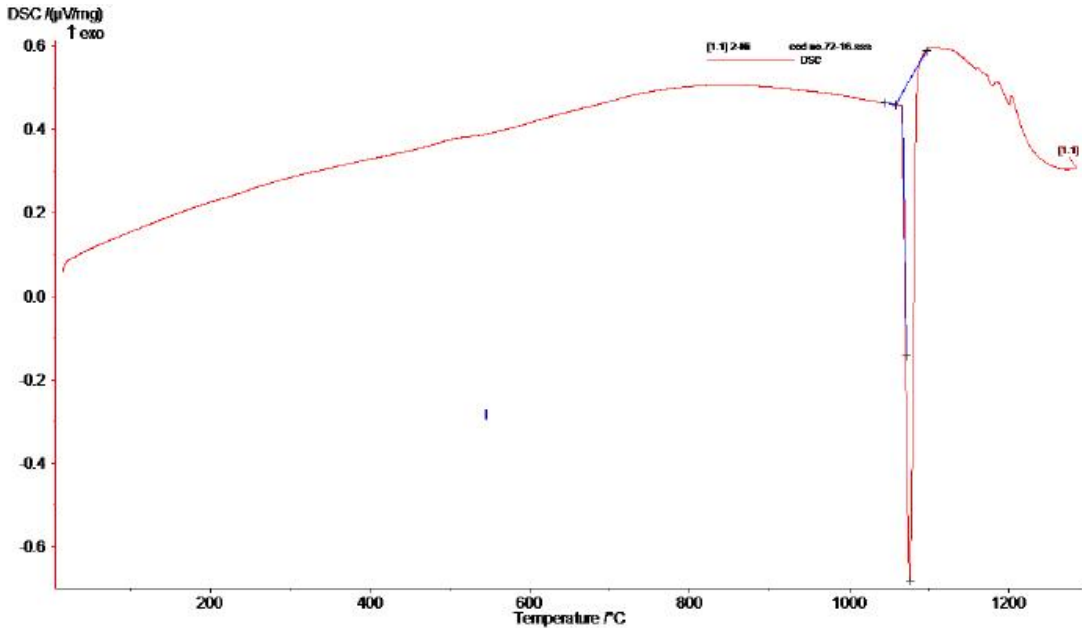

Figure (4f) : DSC thermograph of $Cu_{98}Ni_2$ alloy

or Al or Sn or Ni content and that is agreed with the x-ray diffraction and SEM analysis.

CONCLUSION

Lattice microstrain of copper increased but unit cell volume and crystal size decreased after adding Ge or Mn or Al or Sn or Ni.

Vickers hardness value of copper increased after adding Ge or Mn or Al or Sn or Ni.

Corrosion rate of copper increased after adding Ge or Mn or Al or Sn or Ni.

The melting temperature and thermal behavior of copper changed after adding Ge or Mn or Al or Sn or Ni.

REFERENCES

[1] M.O.Lai, L.Lu, W.H.Lee; J.Mater.Sci., **31(6)**, 1537-1543 **(1996)**.
[2] A.Couture, J.O.Edwards; AFS Trans., **81**, 453-361 **(1973)**.
[3] R.W.Ruddle; Modern Castings, **38**, 81-86 **(1960)**.
[4] A.Cibula; J.Institute of Metals, **82**, 513-523 **(1953)**.
[5] A.Chrysanthou, G.Erbaccio; J.Mat.Sci., **30**, 6339–6344 **(1995)**.
[6] Y.Z.Zhan, G.D.Zhang; Key Eng.Mat., **249**, 227–232 **(2003)**.
[7] K.Ichikawa, M.Achikita; Mat.Trans.JIM, **34**, 718–724 **(1993)**.
[8] R.H Palma, A.O.Sepulveda; Mat.Sci.Forum, **162**, 416-418 **(2003)**.
[9] B.Tiang, P.Liu, K.Song, Y.Li, F.Ren; Mat.Sci.Eng., A, **705**, 435-436 **(2006)**.
[10] Rajković, D.Božić, A.Devečerski; J.Serb.Chem.Soc., **72**, 45–53 **(2007)**.
[11] P.K.Jena, E.A.Brocchi, I.G.Solorzano, M.S.Motta; Mat.Sci.Eng., A, **371**, 72–78 **(2004)**.
[12] J.H.Ahn, I.H.Song, Y.D.Hahn; Mat.Trans.JIM, **37**, 733–737 **(1996)**.
[13] A.Mukhtar, D.L.Zhang, C.Kong, P.Munroe; IOP Conference Series, Mat.Sci.Eng., **4**, 012005 **(2009)**.
[14] S.Timoshenko, J.N.Goddier; "Theory of elasticity, 2nd Ed", McGraw-Hill, New York, 277, **(1951)**.